A STUDY OF ELECTROMAGNETIC RADIATION FROM MONOPOLE ANTENNAS ON SPHERICAL-LOSSY EARTH USING THE FINITE-DIFFERENCE TIME-DOMAIN METHOD

K. Paran and M. Kamyab

Department of Electrical Engineering, K.N.Toosi University of Technology
Tehran, Iran, pkpkp@eetd.kntu.ac.ir - Kamyab@eetd.kntu.ac.ir

(Received: July 26, 2004 – Accepted: October 14, 2004)

Abstract Radiation from monopole antennas on spherical-lossy earth is analyzed by the finite-difference time-domain (FDTD) method in spherical coordinates. A novel generalized perfectly matched layer (PML) has been developed for the truncation of the lossy soil. For having an accurate modeling with less memory requirements, an efficient "non-uniform" mesh generation scheme is used. Also in each time step, computation is limited to that part of the mesh where the radiated pulse is passing (computational window). In this manner, the values of radiated field at far distances can be obtained directly by the FDTD method. The spatial distribution of radiated field and the influence of the ground screen on monopole's admittance are shown in illustrations.

Key Words FDTD Method, Inhomogeneous Media, Electromagnetic Wave Propagation

چکیده با بکارگیری روش تفاضل محدود در حوزه زمان (FDTD) در مختصات کروی، تابش از آنتن های تک-قطبی بر روی زمین کروی دارای تلفات بررسی شده است. برای ختم شبکه، نوعی لایه تطبیقی با توانایی ختم محیط های دارای تلفات ابداع گردید. برای مدلسازی دقیق ساختار با حافظه کامپیوتری کمتر، از نوعی روش شبکه بندی غیریکنواخت استفاده می‌شود. همچنین در هر گام زمانی، محاسبات تنها در بخشی از شبکه که پالس تابشی در حال عبور از آن است (پنجره محاسباتی)، انجام می‌پذیرد. با این تدابیر می‌توان مقادیر میدان را در فواصل دور مستقیماً با شبیه سازی FDTD بدست آورد. در نگاره ها، توزیع مکانی میدان و اثر زمین مصنوعی بر ادمیتانس تک-قطبی نمایش داده شده اند.

1. INTRODUCTION

Since the presentation of the finite-difference time-domain (FDTD) method in 1966 [1], this method has been used for analyzing a broad class of electromagnetic problems including scattering, penetration and absorption of EM waves, coupling and interference, radiating and guiding structures and so on. However, the FDTD method is rarely used for the analysis of propagation problems. In few researches which have been carried out on this subject [2-4], the radiators are considered in the form of vertical or horizontal line sources (not actual antennas) and the earth's surface is assumed to be a perfect electric conductor (PEC) in most cases.

In the present work, radiation from monopole antennas on spherical-lossy earth is analyzed by the FDTD method in spherical coordinates taking the rotational symmetry into account. Up to now some rotational symmetric antennas have been analyzed by 2-D cylindrical FDTD method [5-11], but the radiation of those antennas is taking place either in a homogeneous space or over an infinite-flat PEC ground. Besides, the field values are obtained directly by the FDTD method only in the vicinity of antenna. At far distances, the field values are found by taking the near-to-far-field transformation.

The classical problem of radiating current elements over the earth's surface has been solved rigorously by Sommerfeld back in 1909 [12]. Although it provides a solid basis for

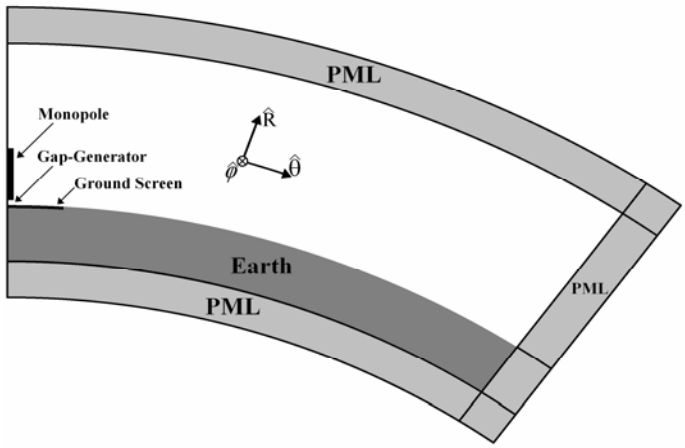

Figure 1. Computational space of the FDTD simulation (figure is not drawn to scale).

understanding various aspects of the propagation phenomenon, the obtained expressions for various field components are quite complex and involved and only approximate numerical versions which were developed later by Norton [13,14] may be used in practical applications. The problem becomes even more difficult to handle for those cases where the dimensions of the radiating antenna are comparable with the wavelength or where the curvature of the earth's surface must be considered. On the contrary, the accurate modeling and simulation of this problem by the FDTD method could provide comprehensive practical results and at the same time it could give physical insight into the propagation process.

The inhomogeneous and lossy nature of this problem, the curvature of the earth's surface and the presence of a propagating mode in the form of surface-wave make the near-to-far-field transformation very difficult and consequently the field values at far distances must be obtained directly by the FDTD method. Therefore the computational space should be extended to far distances, which could lead to a considerable increase in required memory and CPU time. In this work an efficient "non-uniform" mesh generation scheme is used in order to decrease the memory requirements and for having an accurate modeling. Also the excitation is considered in the form of sine carrier modulated by Gaussian pulse (SCMGP) and in each time step, computation is restricted to that part of the mesh where the radiated pulse is passing (computational window). This could considerably reduce the required CPU time. Special mesh truncation technique is needed for the truncation of the lossy-soil at the boundaries of computational space. Therefore a novel generalized perfectly matched layer (PML) has been developed with the capability of truncating inhomogeneous-lossy media [15].

In this article, the key points for performing the above mentioned FDTD analysis are described. Also, the obtained simulation results are presented in the form of graphical illustrations. These illustrations show the spatial distribution of radiated field at a chosen frequency for different types of soil. The influence of the ground screen on monopole's admittance is also shown.

2. FDTD SIMULATION

Figure 1 shows the computational space of the FDTD simulation. The considered structure consists of a quarter-wave monopole over a PEC ground screen (with a radius of $0.25\lambda_0$) on lossy-spherical earth. The exciting source is considered to be a gap-generator between monopole and ground screen. In this rotational symmetric

structure ($\partial/\partial\varphi \equiv 0$) only the rotational symmetric TM modes (E_θ, E_R, H_φ) are excited [5]. The two dimensional (θ, R) model of this structure is surrounded by PML.

2.1 Mesh Generation In order to have an acceptable accuracy especially in calculation of input impedance, the radiating structure should be modeled with a high resolution. Also, since the wavelength in lossy soil is much shorter than the wavelength in air, this part of the computational space must be modeled with finer cells. On the other hand the extension of the computational space to far distances makes it very large especially along the horizontal direction ($\hat{\theta}$ in Figure 1); therefore the remaining parts of the computational space should be modeled with coarse cells in order to keep the memory requirements reasonably low. In this work, an efficient "non-uniform" mesh generation scheme is used which allows us to choose the cell size adaptively in various parts of the computational space and also prevents any sudden change in cell size throughout the mesh. In this manner, the FDTD modeling can be accomplished with an acceptable accuracy and by much less memory requirements.

2.2 Mesh Truncation The truncation of the lossy-soil at the boundaries of computational space requires a special mesh truncation technique. Therefore a novel generalized PML with the capability of truncating inhomogeneous-lossy media has been developed and used. Unlike the other techniques which have been previously proposed for the truncation of lossy media [16-18], this new PML has a very simple formulation and can be easily adapted for different applications.

At those parts of the absorbing layer which are adjacent to specific medium, values of the electric and magnetic characteristics must satisfy the following conditions:

$$\begin{cases} |R_{pm}| = 0 : \forall \vartheta_i \\ \alpha_p = \alpha_m + \Delta\alpha \end{cases} \Leftrightarrow \begin{cases} Z_{C_p} = Z_{C_m} \\ \beta_p = \beta_m \\ \alpha_p = \alpha_m + \Delta\alpha \end{cases}$$

where subscripts "m" and "p" stand for "medium" and "PML" respectively, R_{pm} is the reflection from medium-PML interface, ϑ_i is the incidence angle, α and β are attenuation and phase constants and Z_C is the complex intrinsic impedance. After some mathematical operations the following relations can be obtained for the electric and magnetic characteristics of the PML [15]:

$$\begin{cases} \rho_p = \rho_m + R_m \Delta\alpha \\ \mu_p = \mu_m + X_m \dfrac{\Delta\alpha}{\omega} \\ \sigma_p = \sigma_m + G_m \Delta\alpha \\ \varepsilon_p = \varepsilon_m + B_m \dfrac{\Delta\alpha}{\omega} \end{cases} \quad (1)$$

where

$$\begin{cases} R_m = \mathrm{Re}(Z_{C_m}) \\ X_m = \mathrm{Im}(Z_{C_m}) \\ G_m = \mathrm{Re}(Y_{C_m}) \\ B_m = \mathrm{Im}(Y_{C_m}) \end{cases} \quad (2)$$

The value of $\Delta\alpha$ should be smoothly increased from inner cells of the PML towards outer cells:

$$(\Delta\alpha)_q = (\Delta\alpha)_{\max}\left(\frac{q}{n_p}\right)^{o_p} \quad , \quad q = 1,2,...,n_p \quad (3)$$

Here, n_p is the number of cells along the width of absorbing layer and o_p is the order of the increase (o_p=1 linear, o_p=2 parabolic, etc).

It can be shown that the stability conditions of this PML are as follows [15]:

$$\begin{cases} \dfrac{\sigma_m}{\varepsilon_m} > \dfrac{\rho_m}{\mu_m} : (\Delta\alpha)_{\max} < -\dfrac{\omega\varepsilon_m}{B_m} \\ \dfrac{\sigma_m}{\varepsilon_m} = \dfrac{\rho_m}{\mu_m} : (\Delta\alpha)_{\max} < \infty \\ \dfrac{\sigma_m}{\varepsilon_m} < \dfrac{\rho_m}{\mu_m} : (\Delta\alpha)_{\max} < -\dfrac{\omega\mu_m}{X_m} \end{cases} \quad (4)$$

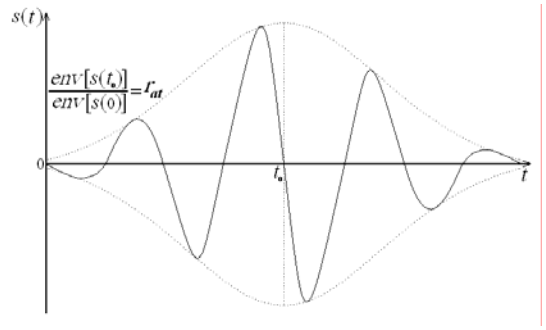

(a)

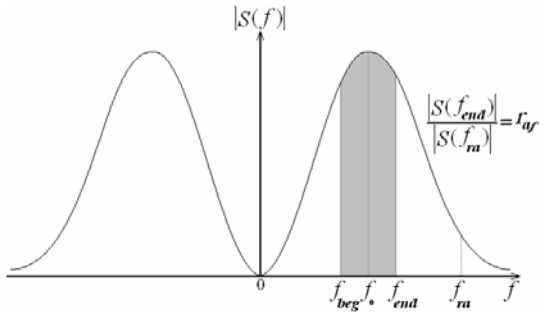

(b)

Figure 2. Sine carrier modulated by Gaussian pulse. (a) Temporal variations. (b) Spectral density.

It should be noted that for lossless media ($\alpha_m = 0$) this PML is reduced to the ordinary PML:

$$\begin{cases} \rho_p = Z_m \Delta\alpha \\ \mu_p = \mu_m \\ \sigma_p = Y_m \Delta\alpha \\ \varepsilon_p = \varepsilon_m \end{cases} \quad (5)$$

2.3 Excitation In this work, the exciting signal is considered in the form of SCMGP with temporal variations and spectral density shown in Figure 2. Unlike the ordinary Gaussian pulse (GP), SCMGP has very small low-frequency content. This is a desirable feature for the FDTD analysis, because significant low-frequency content in the exciting signal can lead to unacceptably long settling times [9]. Also, the spectrum density of SCMGP can be arbitrarily concentrated or distributed around the main frequency (f_0), so it is possible to relatively strengthen the spectrum density at a specified frequency band and weaken it at other frequencies. This increases the accuracy of calculations in the frequency band of interest and reduces the undesired effects of the higher and lower frequencies.

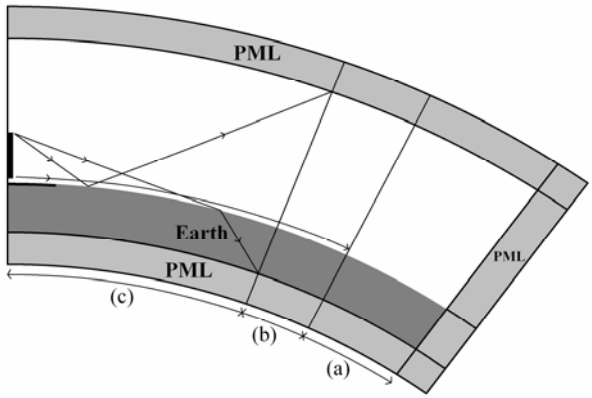

Figure 3. (a) Region beyond the forward part of the radiated pulse. (b) Computational window. (c) Region behind the last reflected or refracted ray leaving the computational space.(Figure is not drawn to scale).

The frequency-domain results can be readily calculated from the time-domain results by taking the discrete Fourier transform. In each simulation, values of the real and imaginary parts of monopole's input admittance are calculated at different frequencies of the specified band (0.8-1.2MHz in this work). Also, the spatial distribution of radiated field is found at a chosen frequency (1MHz in this work).

2.4 Computational Window At each time step, computation is limited to that part of the mesh where the radiated wave is passing ("computational window" in Figure 3). The other parts of the mesh (parts (a) and (c) in Figure 3) are excluded. The front edge of the computational window should always lead the forward part of the radiated pulse and the rear edge should always follow the last reflected or refracted ray of the radiated pulse leaving the computational space. Using the computational window, the required

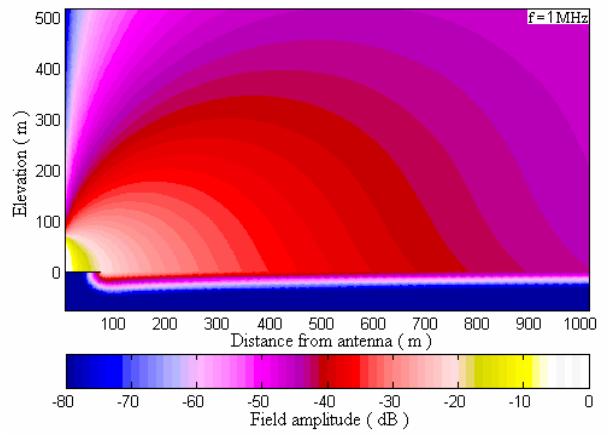

(a)

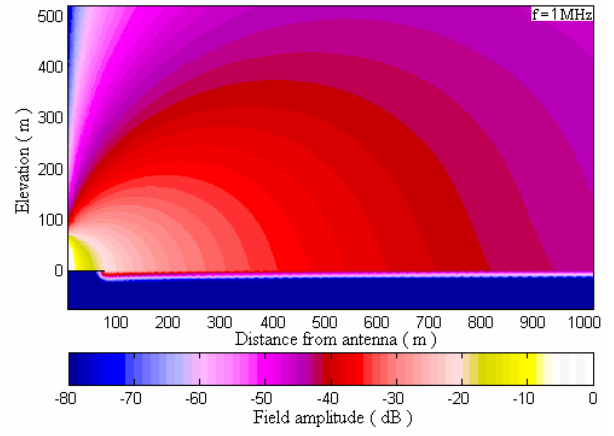

(b)

Figure 4. Spatial distribution of radiated field (amplitude of H_φ). The field distribution is shown up to a distance of 1000m, from 75m below to 500m above the spherical-lossy earth: (a) dry soil and (b) medium soil.

CPU time could be reduced by one order of magnitude.

3. SIMULATION RESULTS

Based on points mentioned in previous sections a FDTD code was developed for the simulation of electromagnetic radiation from monopole antennas

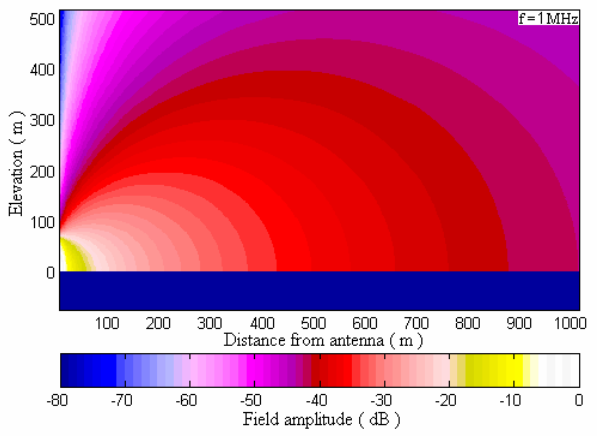

Figure 5. Spatial distribution of radiated field (amplitude of H_φ). The field distribution is shown up to a distance of 1000m, from ground surface to 500m above the spherical-PEC earth.

on spherical-lossy earth. Results are obtained for two types of soil, dry (ε_r = 4, σ = 0.005S/m) and medium (ε_r = 8, σ = 0.02S/m). In this section, some of the results which are obtained by this code (using a Pentium4/2400MHz CPU) are presented.

Figure 4 (a,b) shows the spatial variations of radiated field (amplitude of H_φ) up to a distance of 1000m, from 75m below to 500m above the ground (dry and medium soil, respectively). This figure nicely displays the field distribution around the antenna especially at the edge of the ground screen and below the screen. This figure also shows the attenuation below the earth's surface. For comparison, in Figure 5 the spatial variations of field amplitude above a spherical-PEC earth are shown. Figure 6 shows the distribution of field amplitude up to a distance of 7500m, from 75m below to3500m above the ground. In this figure the formation of the surface-wave (at air-lossy soil interface) and the sky-wave (at higher elevations) is clearly shown (compare this figure with Figure 7 which displays the field distribution above a spherical-PEC earth). About 26MB of memory and 12min of CPU time are needed to perform the FDTD simulation in this case. Figure 8 is the continuation of Figure 6a which shows the

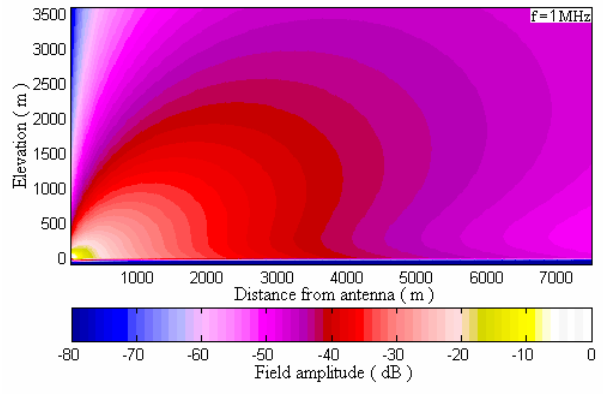

(a)

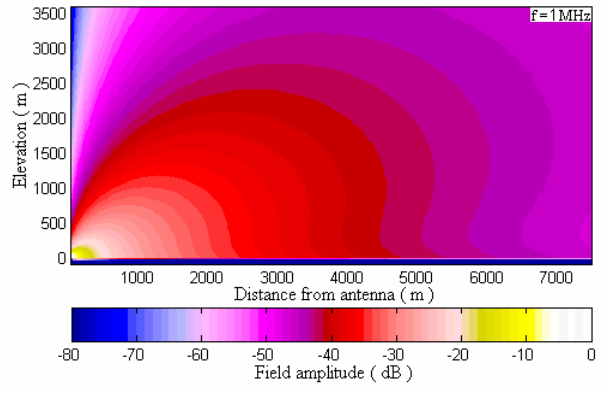

(b)

Figure 6. Spatial distribution of radiated field (amplitude of H_φ). The field distribution is shown up to a distance of 7500m, from ground surface to 3500m above the spherical-lossy earth: (a)dry soil and (b)medium soil.

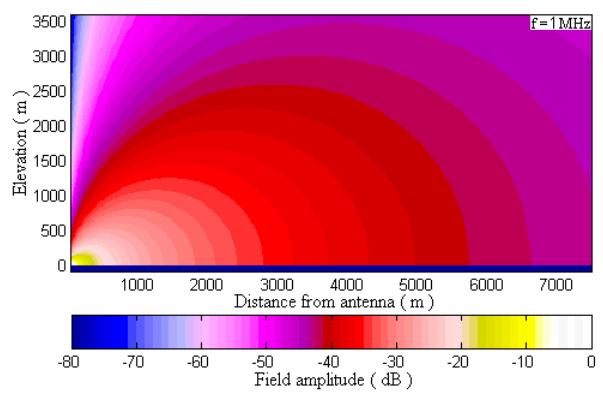

Figure 7. Spatial distribution of radiated field (amplitude of H_φ). The field distribution is shown up to a distance of 7500m, from ground surface to 3500m above the spherical-PEC earth.

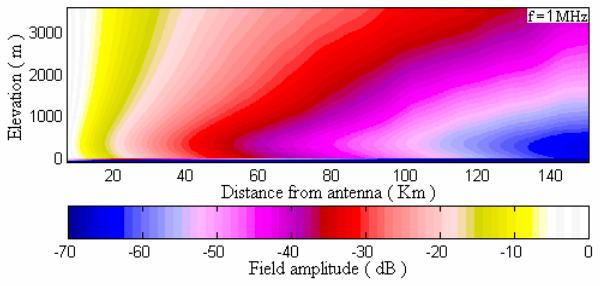

Figure 8. Spatial distribution of radiated field (amplitude of H_φ). The field distribution is shown up to a distance of 150Km, from ground surface to 3500m above the spherical-lossy earth (dry soil).

field distribution from a distance of 7.5Km up to 150 Km ($500\,\lambda_0$). The field values, which were used for drawing this figure, have been obtained directly by the FDTD method. Around 131MB of memory and 340 min of CPU time are required to obtain these values.

The curves in Figure 9 show the real and imaginary parts of monopole's input admittance over the frequency band of 0.8-1.2MHz. The radius of the ground screen is considered to be 75m ($0.25\,\lambda_0$ at 1MHz) and 15m ($0.05\,\lambda_0$ at 1MHz), and the soil below the antenna structure is considered to be dry. It is observed that the input admittance of the monopole antenna could be noticeably affected by the size of the ground screen.

4. CONCLUSIONS

In this research, radiation from monopole antennas on spherical-lossy earth is analyzed by the FDTD method in spherical coordinates taking the rotational symmetry into consideration. A novel generalized PML has been developed and used for the truncation of the lossy soil. Also, an efficient "non-uniform" mesh generation scheme is used in order to decrease the memory requirements and for having an accurate modeling. The exciting signal is considered in the form of SCMGP and in each time

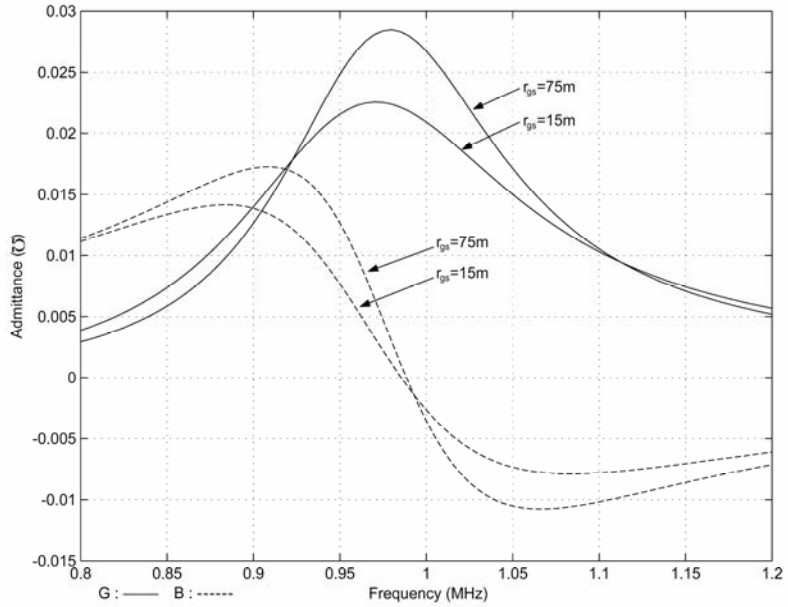

Figure 9. Input admittance of the monopole antenna. The radius of the ground screen is considered to be 75m ($0.25\lambda_0$ at 1MHz) and 15m ($0.05\lambda_0$ at 1MHz) and the soil below the antenna structure is considered to be dry.

step computation is restricted to a "computational window". This could considerably reduce the required CPU time.

Simulation results are presented in the form of graphical illustrations. These illustrations show the spatial distribution of radiated field at a chosen frequency for different types of soil. The influence of the ground screen on monopole's admittance is also shown. The performed simulations show the capabilities of the FDTD method to solve the propagation problems in the case of inhomogeneous-lossy media with curved interfaces. Also it is shown that the values of radiated field at far distances (up to $500\lambda_0$ in this work) can be obtained directly by the FDTD method.

5. ABBREVIATIONS

CPU	Central Processing Unit
EM	Electromagnetic
FDTD	Finite-Difference Time-Domain
GP	Gaussian Pulse
PEC	Perfect Electric Conductor
PML	Perfectly Matched Layer
SCMGP	Sine Carrier Modulated by Gaussian Pulse
TM	Transverse Magnetic

6. SYMBOLS

R, θ, φ	variables in spherical coordinates
E	electric field
H	magnetic field
ε	electric permittivity
ε_r	relative permittivity
μ	magnetic permeability
σ	electric conductivity
ρ	equivalent magnetic conductivity
t	time
f	frequency
ω	angular frequency
λ_0	wavelength in air
R_{pm}	reflection from medium-PML interface
ϑ_i	incidence angle
α	attenuation constant

β	phase constant
Z	intrinsic impedance
Z_C	complex intrinsic impedance
Y	intrinsic admittance
Y_C	complex intrinsic admittance
R	resistance
X	reactance
G	conductance
B	susceptance
n_p	number of cells along the width of absorbing layer
o_p	order of gradual increase of attenuation constant in absorbing layer
$s(t)$	temporal variations of exciting signal
$env[s(t)]$	envelope of $s(t)$
$S(f)$	spectral density of exciting signal
f_{beg}	lowest frequency in the frequency band of interest
f_{end}	highest frequency in the frequency band of interest
f_0	median frequency in the frequency band of interest
f_{ra}	an arbitrary frequency
r_{aff}	desired ratio between $S(f_{end})$ and $S(f_{ra})$
r_{at}	desired ratio between maximum value and starting value of signal's envelope
r_{gs}	radius of ground screen

7. REFERENCES

1. Yee, K. S., "Numerical Solution of Initial Boundary Value Problems Involving Maxwell's Equations in Isotropic Media", ***IEEE Trans. Antennas Propagat.***, Vol. AP-14, No. 3, (1966), 302-307.
2. Cummer, S. A., "Modeling Electromagnetic Propagation in the Earth-Ionosphere Waveguide", ***IEEE Trans. Antennas Propagat.***, Vol. 48, No. 9, (2000), 1420-1429.
3. Akleman, F. and Sevgi, L., "A Novel Finite-Difference Time-Domain Wave Propagator", ***IEEE Trans. Antennas Propagat.***, Vol. 48, No. 3, (2000), 839-841.
4. Sevgi, L., Akleman, F. and Felsen, L. B., "Ground-Wave Propagation Modeling: Problem-Matched Analytical Formulation and Direct Numerical Techniques", ***IEEE Antennas Propagat. Magazine***, Vol. 44, No. 1, (2002), 55-75.
5. Maloney, J. G., Smith, G. S. and Scott J. R., W. R., "Accurate Computation of the Radiation from Simple Antennas Using the Finite-Difference Time-Domain Method", ***IEEE Trans. Antennas Propagat.***, Vol. 38, No. 7, (1990), 1059-1068.
6. Maloney, J. G. and Smith, G. S., "A Study of Transient Radiation from the Wu-King Resistive Monopole–FDTD Analysis and Experimental Measurements", ***IEEE Trans. Antennas Propagat.***, Vol. 41, No. 5, (1993), 668-676.
7. Maloney, J. G. and Smith, G. S., "Optimization of a Conical Antenna for Pulse Radiation: An Efficient Design Using Resistive Loading", ***IEEE Trans. Antennas Propagat.***, Vol. 41, No. 7, (1993), 940-947.
8. Montoya, T.P. and Smith, G. S., "A Study of Pulse Radiation from Several Broad-Band Monopoles", ***IEEE Trans. Antennas Propagat.***, Vol. 44, No. 8, (1996), 1172-1182.
9. Hertel, J. W. and Smith, G. S., "The Insulated Linear Antenna", ***IEEE Trans. Antennas Propagat.***, Vol. 48, No. 6, (2000), 914-920.
10. Shum, S. M. and Luk, K. M., "Characteristics of Dielectric Ring Resonator Antenna with an Air Gap", ***Electronics Letters***, Vol. 30, No. 4, (1994), 277-278.
11. Shum, S. M. and Luk, K. M.,"Stacked Annular Ring Dielectric Resonator Antenna Excited by Axi-Symmetric Coaxial Probe", ***IEEE Trans. Antennas Propagat.***, Vol. 43, No. 8, (1995), 889-892.
12. Sommerfeld, A. N., "Propagation of Waves in Wireless Telegraphy", ***Ann. Phys. (Leipzig)***, Vol. 28, (1909), 665-736.
13. Norton, K. A., "The Propagation of Radio Waves over the Surface of the Earth and in the Upper Atmosphere", ***Proc. IRE***, Vol. 24, (1936), 1367-1387.
14. Norton, K. A., "The Propagation of Radio Waves over the Surface of the Earth and in the Upper Atmosphere", ***Proc. IRE***, Vol. 25, (1937), 1203-1236.
15. Paran, K. and Kamyab, M., "Generalized Perfectly Matched Layer for the Truncation of Lossy Media", Submitted for publication.
16. Fang, J. and Wu, Z., "Generalized Perfectly Matched Layer for the Absorption of Propagating and Evanescent Waves in Lossless and Lossy Media", ***IEEE Trans. Microwave Theory Tech.***, Vol. 44, No. 12, (1996), 2216-2222.
17. Wittwer, D. C. and Ziokowski, R. W., "Two Time-Derivative Lorentz Material (2TDLM) Formulation of a Maxwellian Absorbing Layer Matched to a Lossy Medium", ***IEEE Trans. Antennas Propagat.***, Vol. 48, No. 2, (2000), 192-199.
18. Lazzi, G., Gandhi, O. P. and Sullivan, D. M., "Use of PML Absorbing Layers for the Truncation of the Head Model in Cellular Telephone Simulations", ***IEEE Trans. Antennas Propagat.***, Vol. 48, No. 11, (2000), 2033-2039.